Self-bound droplets in bosonic atomic gases

Luca Salasnich

Dipartimento di Fisica e Astronomia "Galileo Galilei" and Padua Qtech, Università di Padova
INFN, Sezione di Padova
INO-CNR, Research Unit of Sesto Fiorentino

International Workshop on Atomic Physics,
Max Planck Institute for the Physics of Complex Systems
Dresden, November 26, 2025

Collaboration with G.F. Bertacco, A. Cappellaro, and T. Macri

Summary

- Self-bound Bose-Bose droplets
- Beyond-mean-field effective action
- Gaussian ansatz and soliton-droplet crossover
- Breathing modes
- Spin-dipole mode
- Bose-Bose mixture with Rabi coupling
- Conclusions

Self-bound Bose-Bose droplets

- In 2015 Dmitry Petrov suggested theoretically[1] the existence of self-bound quantum droplets in an attractive Bose-Bose mixture, where the collapse is suppressed by a beyond-mean-field term.
- Experiments with two internal states of ^{39}K atoms in a 3D configuration, performed both at Barcelona[2] and Florence[3], confirmed these theoretical predictions.
- In another experiment at Barcelona[4] self-bound states of the two-component BEC were studied in a **tight optical waveguide** (quasi-1D confinement): a smooth crossover interpolating between bright soliton and droplet states has been observed.
- In 2019 at LENS (Florence) there was the observation of quantum droplets in a ^{87}Rb-^{41}K heteronuclear bosonic mixture.[5]

[1] D.S. Petrov, Phys. Rev. Lett. **115**, 155302 (2015).
[2] C.R. Cabrera *et al.*, Science **359**, 6373 (2018).
[3] G. Semeghini *et al.*. Phys. Rev. Lett. **120**, 235301 (2018)
[4] P. Cheiney *et al.*, Phys. Rev. Lett. **120** 135301 (2018).
[5] C. D'Errico *et al*, Phys. Rev. Res. **1**, 033155 (2019).

Beyond-mean-field effective action (I)

We consider a Bose gas made of atoms in two different hyperfine states. Each component can be described by a complex field $\psi_j(\mathbf{r}, t)$ $(j = 1, 2)$, whose dynamics results from the following real-time low-energy effective action

$$S = \int dt\, d^3\mathbf{r} \Big[\sum_{j=1,2} \frac{i\hbar}{2} \big(\psi_j^* \partial_t \psi_j - \psi_j \partial_t \psi_j^*\big) - \mathcal{E}_{\text{tot}}\big(\psi_1, \psi_2\big) \Big] \,. \qquad (1)$$

The total energy density $\mathcal{E}_{\text{tot}}$ reads

$$\mathcal{E}_{\text{tot}} = \sum_{j=1,2} \left[\frac{\hbar^2}{2m} |\nabla \psi_j|^2 + V_{\text{ext}}(\mathbf{r}) |\psi_j|^2 + \frac{1}{2} g_{jj} |\psi_j|^4 \right] + g_{12} |\psi_1|^2 |\psi_2|^2 + \mathcal{E}_{\text{BMF}}(\psi_1, \psi_2) \,, \qquad (2)$$

where $V_{\text{ext}}(\mathbf{r})$ is an external confining potential, $g_{jk} = 4\pi\hbar^2 a_{jk}/m$ are the interaction strengths with a_{jk} being intra- and inter-species scattering lengths, and $n_j(\mathbf{r}, t) = |\psi_j(\mathbf{r}, t)|^2$ is the number density of the species j.

Beyond-mean-field effective action (II)

The beyond-mean-field term $\mathcal{E}_{\text{BMF}}$ arises from the zero-point energy of Bogoliubov elementary excitations[6], namely

$$\mathcal{E}_{\text{BMF}} = \frac{8}{15\pi^2}\left(\frac{m}{\hbar^2}\right)^{3/2}(g_{11}n_1)^{5/2} f\left(\frac{g_{12}^2}{g_{11}g_{22}}, \frac{g_{22}n_2}{g_{11}n_1}\right) \tag{3}$$

with $f(x,y) = \sum_{\pm}[1 + y \pm \sqrt{(1-y)^2 + 4xy}]^{5/2}/(4\sqrt{2})$.
The calculation leading to the ground state properties can be simplified by assuming[7] the two components occupying the same spatial mode $\phi(\mathbf{r}, t)$. The bosonic fields can then be written as

$$\psi_j(\mathbf{r}, t) = \sqrt{N_j}\ \phi(\mathbf{r}, t)\ . \tag{4}$$

This assumption neglects the inter-component dynamics, resulting inadequate to probe spin-dipole oscillations.

---

[6] D.M. Larsen, Ann. Phys. 24, 89 (1963).

[7] D.S. Petrov, Phys. Rev. Lett. **115**, 155302 (2015); D.S. Petrov and G.E. Astrakharcik, Phys. Rev. Lett. **117**, 100401 (2016).

Beyond-mean-field effective action (III)

We work under the condition

$$\frac{N_1}{N_2} = \sqrt{\frac{a_{22}}{a_{11}}} \; , \qquad (5)$$

which comes from the minimization of the mean-field energy density for the uniform system.[8] By defining[9]

$$\Delta a = a_{12} + \sqrt{a_{11} a_{22}} \quad \text{with} \quad a_{11} > 0, a_{22} > 0 \; , \qquad (6)$$

the total energy density reads (with $N = N_1 + N_2$)

$$\begin{aligned} \frac{\mathcal{E}_{\text{tot}}}{N} &= \frac{\hbar^2}{2m} \left|\nabla \phi\right|^2 + V_{\text{ext}}(\mathbf{r}) \left|\phi\right|^2 + N \frac{4\pi\hbar^2}{m} \frac{\Delta a \sqrt{a_{22}/a_{11}}}{\left(1 + \sqrt{a_{22}/a_{11}}\right)^2} \left|\phi\right|^4 \\ &+ N^{3/2} \frac{256\sqrt{\pi}\hbar^2}{15m} \left(\frac{\sqrt{a_{11} a_{22}}}{1 + \sqrt{a_{22}/a_{11}}}\right)^{5/2} f\left(\frac{a_{12}^2}{a_{11} a_{22}}, \sqrt{\frac{a_{22}}{a_{11}}}\right) \left|\phi\right|^5 \; . \end{aligned} \qquad (7)$$

[8] D.S. Petrov, Phys. Rev. Lett. **115**, 155302 (2015).

[9] Notice that the mean-field uniform system becomes unstable for $\Delta a < 0$.

Beyond-mean-field effective action (IV)

Inspired by the experiment of the Tarruell group at Barcelona[10] with ^{39}K atoms, we study a quasi-1D optical waveguide which gives a harmonic confinement **only** on a transverse plane

$$V_{\text{ext}}(\mathbf{r}) = \frac{1}{2} m\omega_{\perp}^2 (x^2 + y^2) \, . \tag{8}$$

The presence of a harmonic potential defines a characteristic length scale, namely

$$a_{\perp} = \sqrt{\frac{\hbar}{m\omega_{\perp}}} \, . \tag{9}$$

We work with $a_{11} > 0$, $a_{22} > 0$ **but** $a_{12} < 0$. We investigate different values of

$$\Delta a = a_{12} + \sqrt{a_{11} a_{22}} \tag{10}$$

in the regime where $\Delta a < 0$, namely in the regime where $a_{12} < -\sqrt{a_{11} a_{22}}$.

[10] P. Cheiney *et al.*, Phys. Rev. Lett. **120** 135301 (2018).

Gaussian ansatz and soliton-droplet crossover (I)

The properties of the system can be analytically explored by taking a Gaussian variational ansatz

$$\phi(\mathbf{r}) = \frac{1}{\pi^{3/4}\sigma_\rho \sigma_z^{1/2}} \exp\left(-\frac{x^2+y^2}{2\sigma_\rho^2} - \frac{z^2}{2\sigma_z^2} \right) , \tag{11}$$

whose variational parameters are σ_ρ and σ_z.

By replacing Eq. (11) in the total energy density, the variational energy per particle is then given by

$$\frac{E}{N\hbar\omega_\perp} = \frac{1}{4}\left(\frac{2}{\sigma_\rho^2} + \frac{1}{\sigma_z^2}\right) + \frac{\sigma_\rho^2}{2} + \frac{2N\Delta a}{\sqrt{2\pi}\sigma_\rho^2\sigma_z} \frac{\sqrt{a_{22}/a_{11}}}{\left(1+\sqrt{a_{22}/a_{11}}\right)^2}$$
$$+ \frac{512\sqrt{2}}{75\sqrt{5}\pi^{7/4}} \frac{N^{3/2}}{(\sigma_\rho^2\sigma_z)^{3/2}} \left(\frac{\sqrt{a_{11}a_{22}}}{1+\sqrt{a_{22}/a_{11}}}\right)^{5/2} f\left(\frac{a_{12}^2}{a_{11}a_{22}}, \sqrt{\frac{a_{22}}{a_{11}}}\right) . \tag{12}$$

Here the lengths are in units of $a_\perp$.

Experimentally, by means of Feshbach resonance, below a critical value of the external magnetic field, the condition $\Delta a < 0$ is achieved.

Gaussian ansatz and soliton-droplet crossover (II)

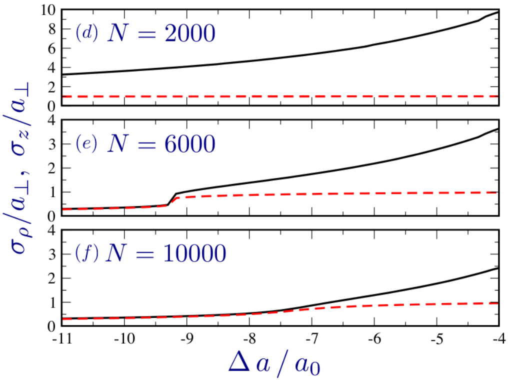

Axial width σ_z (**black solid curve**) and transverse width σ_ρ (**red dashed curve**) as a function of $\Delta a = a_{12} + \sqrt{a_{11}a_{22}}$, for three values of the particle number N in the ^{39}K-^{39}K mixture. We set $a_{11} = a_{22} = 33.5a_0$ and use $a_{12} < 0$. a_0 is the Bohr radius. **The self-bound spherical droplet is obtained when** $\sigma_\rho = \sigma_z$.[11]

[11] A. Cappellaro, T. Macri, and LS, Phys. Rev. A **97**, 053623 (2018).

Breathing modes (I)

A deeper insight into the differences between solitonic and droplet states can be reached by examining collective excitations around the minima of the Gaussian variational energy.
Thus, we adopt a time-dependent Gaussian variational ansatz for the complex scalar field:

$$\phi(\mathbf{r},t) = \sqrt{\frac{1}{\pi^{3/2}\prod_{K=x,y,z}\sigma_K(t)}}\exp\left(\sum_{K=x,y,z}\left(-\frac{K^2}{2\sigma_K(t)^2}+i\beta(t)K^2\right)\right). \tag{13}$$

Inserting this ansatz into the beyond-mean-field effective action, after some manipulations we obtain a new effective action for the three time-dependent variational widths $\sigma_K(t)$.
From the corresponding linearized Euler-Lagrange equations we find three collective frequencies: two (quasi-degenerate) frequencies are related to a breathing oscillation in the $x-y$ plane while the third frequency is related to a beathing along the z axis.

Breathing modes (II)

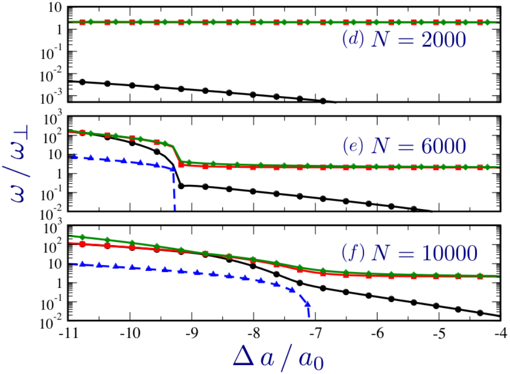

Breathing frequencies (**red**, **green** and **black** curves) as a function of $\Delta a = a_{12} + \sqrt{a_{11} a_{22}}$, for three values of the particle number N in the ^{39}K-^{39}K mixture with $a_{11} = a_{22} = 33.5 a_0$ and $a_{12} < 0$. The **blue curve** is $-\mu/\hbar$, with μ the chemical potential for $\mu < 0$ (quantum droplet regime).[12]

[12] A. Cappellaro, T. Macri, and LS, Phys. Rev. A **97**, 053623 (2018).

Spin-dipole mode (I)

We now consider the oscillatory motion occurring when there is a displacement $\bar{z}_1(t) - \bar{z}_2(t)$ along the z axis of the centers of mass $\bar{z}_j(t)$ of the two bosonic components.

To model this spin-dipole collective dynamics, we go beyond the assumption where the two components occupy the same spatial mode.

The corresponding Gaussian variational ansatz is given by

$$\psi_j(\mathbf{r}, t) = \sqrt{\frac{N_j}{\pi^{3/2} \prod_{K=x,y,z} \sigma_K(t)}} \times \exp\left[\sum_{K=x,y,z} \left(-\frac{(K - \bar{z}_j(t)\delta_{K,z})^2}{2\sigma_{K,j}(t)^2} + i\alpha_j(t) z + i\beta_{K,j}(t) K^2 \right) \right],$$

where the fields $\psi_j(\mathbf{r}, t)$ are normalized to N_j.

Spin-dipole mode (II)

We insert the time-dependent variational ansatz for the two fields $\psi_j(\mathbf{r}, t)$ into the beyond-mean-field effective action, which becomes a functional of the variational parameters.
After several manipulations, we find that $\tilde{z}(t) = z_1(t) - z_2(t)$ satisfies the equation

$$\frac{d^2}{dt^2}\tilde{z}(t) + \omega_{sd}^2\,\tilde{z}(t) = 0 \,, \tag{14}$$

where the spin-dipole frequency ω_{sd} of the relative motion of the two bosonic clouds reads

$$\frac{\omega_{sd}^2}{\omega_\perp^2} = -\sqrt{\frac{8}{\pi}}\,\frac{N_1\left(a_{12}/a_\perp\right)}{\sigma_{\rho,0}^2\sigma_{z,0}^3} + \frac{2048}{25\pi^{1/4}}\,\frac{(a_{11}/a_\perp)^{5/2}N_1^{3/2}}{\sigma_{\rho,0}^2\sigma_{z,0}^{7/2}} \,, \tag{15}$$

where $\sigma_{\rho,0}$ and $\sigma_{z,0}$ are the equilibrium values, and assuming $N_1 = N_2$.

Spin-dipole mode (III)

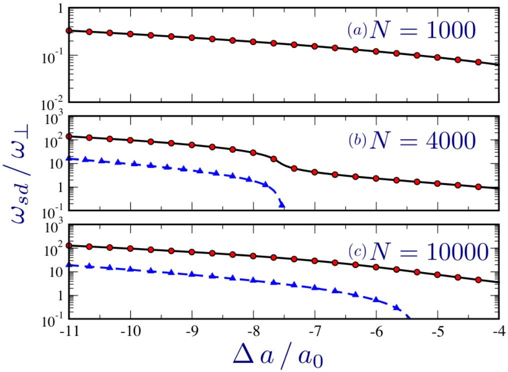

Spin-dipole frequency (black curve with red dots) as a function of $\Delta a = a_{12} + \sqrt{a_{11} a_{22}}$, for three values of the particle number N in the ^{39}K-^{39}K mixture with $a_{11} = a_{22} = 33.5 a_0$ and $a_{12} < 0$. The **blue curve** is $-\mu/\hbar$ for $\mu < 0$.[13]

[13] A. Cappellaro, T. Macri, and LS, Phys. Rev. A **97**, 053623 (2018).

Bose-Bose droplets with Rabi coupling (I)

Let us consider again a bosonic gas is characterized by two-hyperfine components with bosonic complex fields $\psi_j(\mathbf{r}, t)$, $j = 1, 2$. The Lagrangian density of the system reads

$$\begin{aligned}\mathcal{L} &= \sum_{j=1,2} \left[i\hbar\psi_j^* \partial_t \psi_j - \frac{\hbar^2}{2m} |\nabla\psi_j|^2 - \frac{g}{2} |\psi_j|^4 \right] - g_{12} |\psi_1|^2 |\psi_2|^2 \\ &+ \hbar\omega_R \left[\psi_1^* \psi_2 + \psi_2^* \psi_1 \right] . \end{aligned} \quad (16)$$

In addition to the usual intra-species ($g = g_{11} = g_{22}$) and inter-species (g_{12}) contact interactions, atoms with mass m in different hyperfine states interact also via an external coherent Rabi coupling of frequency ω_{R}, which drives an exchange of atoms between the two components.

Bose-Bose droplets with Rabi coupling (II)

The presence of the Rabi coupling implies that only the total number

$$N = N_1(t) + N_2(t) \tag{17}$$

of atoms is conserved, with

$$N_j(t) = \int |\psi_j(\mathbf{r}, t)|^2 \, d^3\mathbf{r} \tag{18}$$

the number of atoms in the j-th hyperfine component ($j = 1, 2$).
In 2013 the existence and stability of the symmetric ground state with $N_1 = N_2$ was discussed by Abad and Recati[14]. In addition to the symmetric configuration, a ground state with non-zero population imbalance is also possible[15]

[14] M. Abad and A. Recati, Eur. Phys. J. D **67** (7), 148 (2013).
[15] C. P. Search, A. G. Rojo, and P. R. Berman, Phys. Rev. A **64**, 013615 (2001).

Bose-Bose droplets with Rabi coupling (III)

At the mean-field level, for the **symmetric and uniform ground state**, characterized by $n_1 = n_2 = n/2$, the chemical potential μ reads

$$\mu = \frac{1}{2} g n (1 + \epsilon) - \hbar \omega_{\mathrm{R}} \ , \tag{19}$$

where $n = N/L^2$ is the 2D total number density of bosons, with $g > 0$ and $\epsilon = g_{12}/g$.

This mean-field **symmetric and uniform ground state** is stable under the conditions[16]

$$g + g_{12} > 0 \qquad \text{and} \qquad (g - g_{12}) n + 2\hbar\omega_{\mathrm{R}} > 0 \ , \tag{20}$$

namely

$$-1 < \epsilon < 1 + \frac{2\hbar\omega_{\mathrm{R}}}{gn} \ . \tag{21}$$

[16] M. Abad and A. Recati, Eur. Phys. J. D **67** (7), 148 (2013).

Bose-Bose droplets with Rabi coupling (IV)

The Bogoliubov spectrum of elementary excitations of the uniform system has two branches, given by

$$E_k^{(-)} = \sqrt{\frac{\hbar^2 k^2}{2m}\left[\frac{\hbar^2 k^2}{2m} + 2(\mu + \hbar\omega_{\rm R})\right]}\ , \quad (22)$$

$$E_k^{(+)} = \sqrt{\frac{\hbar^2 k^2}{2m}\left[\frac{\hbar^2 k^2}{2m} + 2A\right] + B}\ , \quad (23)$$

where μ is the chemical potential. Moreover the two parameters appearing in the gapped branch are

$$A = \frac{1}{2}gn(1-\epsilon) + 2\hbar\omega_{\rm R}\ , \quad (24)$$

$$B = 4\hbar\omega_{\rm R}\left[\frac{1}{2}gn(1-\epsilon) + \hbar\omega_{\rm R}\right]\ , \quad (25)$$

again with $\epsilon = g_{12}/g$ and $g = g_{11} = g_{22}$.

Bose-Bose droplets with Rabi coupling (V)

Remember that we set

$$\epsilon = g_{12}/g = a_{12}/a \tag{26}$$

with a the intra-component scattering length and a_{12} the inter-component scattering length. We also introduce

$$\bar{n} = na^3 \tag{27}$$

that is our gas parameter. We use the elementary excitations to obtain the beyond-mean-field one-loop (Gaussian) corrections to the mean-field energy. In particular, we find[17]

$$\begin{aligned} \frac{\mathcal{E}}{E_B/a^3} &= \pi\left(1+\epsilon\right)\bar{n}^2 - \bar{\omega}_R\bar{n} + \frac{8}{15\pi^2}\left[2\pi\bar{n}(1+\epsilon)\right]^{5/2} \\ &+ \frac{8}{15\pi^2}\left[2\pi\bar{n}(1-\epsilon)\right]^{5/2} + \frac{14}{3\pi^2}\bar{\omega}_R\left[2\pi\bar{n}(1-\epsilon)\right]^{3/2}, \end{aligned} \tag{28}$$

where $E_B = \hbar^2/ma^2$ and $\bar{\omega}_R = \hbar\omega_R/E_B$.

[17] A. Cappellaro, T. Macri, G. F. Bertacco, and LS, Sci. Rep. **7**, 13358 (2017).

Bose-Bose droplets with Rabi coupling (VI)

Notice that in Eq. (28) for $\bar{\omega}_R = 0$ one recovers the Larsen's zero-temperature equation of state[18]
Moreover, from Eq. (28) one finds that for $|\epsilon| > 1$ the uniform configuration is not stable. If $\epsilon > 1$, at the mean field level, one expects phase separation or population imbalance.[19]
Instead, if $\epsilon < -1$ the term proportional to $[(1+\epsilon)\bar{n}]^{5/2}$ becomes imaginary and it gives rise to a dissipative dynamics. However, this dissipative term can be neglected if $\bar{n}$ is not too large. In this way, by minimization of the energy density of Eq. (28), for $\epsilon < -1$ we obtain

$$\bar{n}_{\min} = \left(\frac{5\sqrt{\pi}|1+\epsilon|}{32\sqrt{2}(1+|\epsilon|)^{5/2}} \left[1 + \sqrt{1 - \frac{1792\,\bar{\omega}_R}{15\pi^2} \frac{(1+|\epsilon|)^4}{|1+\epsilon|^2}} \right] \right)^2 . \quad (29)$$

as a local minimum, if $\bar{\omega}_R < \bar{\omega}_c = \frac{15\pi^2}{1792} \frac{|1+\epsilon|^2}{(1+|\epsilon|)^4}$. For larger $\bar{\omega}_R$ there is only the absolute minimum with zero energy at $\bar{n} = 0$.

[18] D.M. Larsen, Ann. Phys. 24, 89 (1963).
[19] K. Furutani, A. Perali, and LS, Phys. Rev. A **107**, L041302 (2023).

Bose-Bose droplets with Rabi coupling (VII)

The local minimum $\bar{n}_{\rm min}$ we found for $\epsilon < -1$ and $\bar{\omega}_R < \bar{\omega}_c = \frac{15\pi^2}{1792} \frac{|1+\epsilon|^2}{(1+|\epsilon|)^4}$ suggests the existence of a Bose-Bose-droplet also in the presence of Rabi coupling.

To get more info about this Bose-Bose droplet with Rabi we consider a space-time dependent complex field $\Psi(\mathbf{r}, t)$ such that $n(\mathbf{r}, t) = \left|\Psi(\mathbf{r}, t)\right|^2$ is the space-time dependent total number density, and clearly $N = \int d^3\mathbf{r}\ n(\mathbf{r}, t)$. The dynamics of $\Psi(\mathbf{r}, t)$ is driven by the following real-time effective action

$$S_{\rm eff}[\Psi^*, \Psi] = \int dt\, d^3\mathbf{r} \left[i\hbar\Psi^*\partial_t\Psi - \frac{\hbar^2\left|\nabla\Psi\right|^2}{2m} - \mathcal{E}_{ND}\left(|\Psi|^2\right)\right], \qquad (30)$$

where the non-dissipative (ND) energy density $\mathcal{E}_{ND}$ is derived from Eq. (28) neglecting the imaginary term proportional to $[(1+\epsilon)\bar{n}]^{5/2}$.

Bose-Bose droplets with Rabi coupling (VIII)

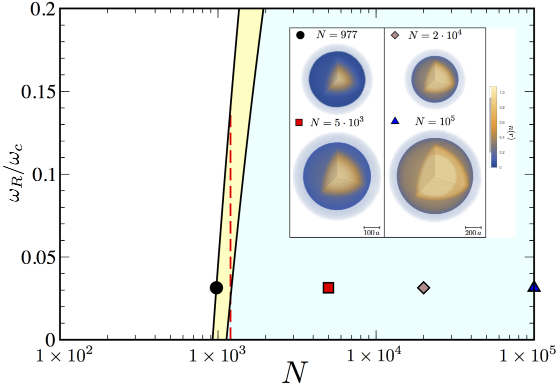

Phase diagram for the Bose-Bose droplet with Rabi coupling: unstable (white region), metastable (yellow region), stable (light blue region). We choose ^{39}K atoms with $N_1 = N_2 = N$, $a = 40a_0$ with a_0 the Bohr radius, and $\epsilon = -1.5$, which implies $\omega_c/(2\pi) = 31.8$ kHz. Red dashed line refers to a system of $N = 1200$ particles.

Bose-Bose droplets with Rabi coupling (IX)

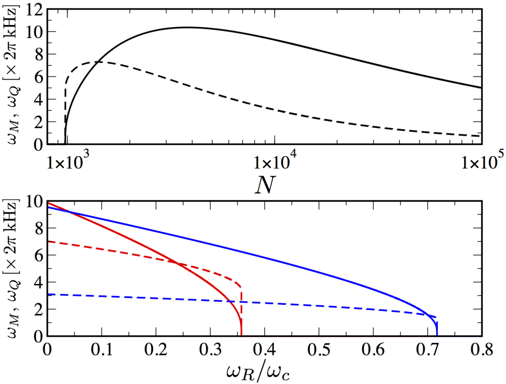

Upper panel: monopole (breathing) mode frequency ω_M (solid) and quadrupole mode frequency ω_Q (dashed) of the Bose-Bose droplet as a function of particle number, with $\omega_R/2\pi = 1$ kHz, $a = 40a_0$, and $\epsilon = -1.5$. Below $N \simeq 977$ the droplet becomes unstable. Lower panel: frequencies as a function of Rabi coupling for $N = 2 \cdot 10^3$ (red), and $N = 10^5$ (blue). The critical Rabi frequency occurs at $\omega_c/(2\pi) = 31.8$ kHz.

Conclusions

- We have analyzed a two-component BEC with attractive interparticle interactions along the crossover from soliton to self-bound droplets in a quasi one dimensional waveguide.
- We have found a sharp difference of the collective modes in the two regimes:
  – in the soliton regime: two distinguishable collective frequencies;
  – deep into the spherical droplet regime: only one breathing frequency (triple degenerate).
- Also the spin-dipole mode can be excited, and we have found an analytical formula for it.
- The inclusion of a Rabi coupling modifies the properties of the two-component quantum droplet.

Acknowledgements

Thank you for attention!

Main sponsors:
– MUR-PRIN 2022 "Quantum Atomic Mixtures: Droplets, Topological Structures, and Vortices".
– INFN Iniziativa Specifica "Quantum".
– Dipartimenti di Eccellenza MUR 2023-2027 "Frontiere Quantistiche", DFA UNIPD.
– National Center for HPC, the Big Data and Quantum Computing [Spoke 10: Quantum Computing].